Influence of Joints between Steel Plates on Load-Carrying Capacity of Reinforced Concrete Girders Strengthened with Externally Bonded Steel Plates

Eiji Yoshida[1], Jun Murakoshi[1], Yoshitomi Kimura[2], Yoshiki Tanaka[1]

Abstract

Single-spliced adhesive joints are used on steel plates to strengthen reinforced concrete girders on highway bridges having externally bonded steel plates. When we conducted load-carrying capacity tests on reinforced concrete beams having externally bonded steel plates after 75 years of service, the expected load-carrying capacity was not obtained due to joint debonding. In order to understand the effect of joints on load-carrying capacity and failure properties of reinforced concrete girders strengthened with externally bonded steel plates, a stress-strain relation model for joints was applied to the numerical calculation using the multi-cross section method to compare the calculated values with experimental results. Results revealed that a decline in rigidity of girders after partial debonding of the splice plate of a joint can usually be well expressed by applying a model and that the maximum load is capped even if the joint strength is improved due to effects from eccentricity specific to a single-spliced joint structure.

Introduction

Some reinforced concrete (RC) girders and decks of currently used for highway bridges have been strengthened by adhesively bonding steel plates or fiber reinforced polymer (FRP) sheets to them in order to increase the design load pursuant to amendment of the Road Structure Ordinance or to correct for insufficient load-carrying capacity caused by deterioration over time(Photo 1). Ensuring effective use of these bridges requires precisely evaluating the behavior and load-carrying capacity of the strengthened members.

While strengthening by use of FRP sheets has spread in recent years, there are still currently many structures bonded with steel plates, so a precise grasp of the effect from strengthening by steel plate bonding as well as FRP bonding is required. There have been numerous reports of studies that are primarily experimental studies, on the steel plate bonding method[1]). In studies focusing on problems of reinforced concrete girders strengthened with steel plates bonded to their soffit, there are cases where the specified strengthening effect cannot be obtained due to plate end debonding failure occurring from the effects of highly localized vertical stress and shear stress(Figure 1 (a)).

Adhesive single-sided splice joints are used between steel plates to strengthen the reinforced concrete girders in currently used highway bridges having externally bonded steel plates. When we conducted load-carrying capacity test on reinforced concrete beams

---

[1] Center for Advanced Engineering Structural Assessment and Research, Public Works Research Institute, Japan
[2] National Institute for Land and Infrastructure Management, Japan

with externally bonded steel plates that had been in service for 75 years, we found that the expected load-carrying capacity was not obtained due to debonding of these joints[2], [3].

In order to understand the effect of joints on the load-carrying capacity and the failure properties of reinforced concrete girders strengthened with externally bonded steel plates, a model of the stress-strain relation for the joints was applied to the numerical calculation using the multi-cross section method to compare the calculated values with the experimental results.

Specimens

Table 1 is the list of specimens. Figures 2 and 3 respectively show the appearance of specimens S1 to S4 before and after the loading test and cross sections of specimens S3 and S4 after the test. Since the webs of the four reinforced concrete beams were partially covered with coating, this was removed before inspection. Extensive cracks on the sides of the webs of specimens S2 and S4 were found compared with those of specimens S1 and S3; and cracks along the lower main reinforcing bar were confirmed on the sides of the webs of specimens S2 and S4.

Innumerable horizontal cracks were found on the sides of the specimens S1 through S4 decks. In addition, inspection of their cross section after the loading test revealed significant cracks on the deck section. A hammer sounding survey to test for debonding revealed it occurred across all of specimen S4 and extensively on specimens S2 and S3. A dissection survey found two 8 mm diameter stirrups at intervals of approximately 200 mm.

Two joints are single-sided adhesive joints using adhesive. In specimens S3 and S4, one-sided bolts (hereinafter "bolts") were inserted in this area and an axial force (axial force is equivalent to 131kN, F8T by catalog specifications) was applied to them (Figure 4). Bolts were located near the anchor where they did not interfere with the main reinforcing bar. After an axial force was applied to the bolts, epoxy resin adhesive was injected into the bolt holes from the drilled web side (diameter: 6 mm). The temporal change in bolt axial tension was measured by the strain at the end of bolt shank which has a proportional relation to the axial force. The average axial tension of the bolts on the specimens S3 and S4 on the day before the test was 125 kN and 107 kN each.

Survey of materials Properties

Concrete

Figure 5 shows results of the compressive strength test of the concrete cores. Concrete cores were sampled from the web side of the beam of specimens S1 and S2 and the cross section of specimens S3 and S4 in the axial direction.

The results of the test for specimen S2 were plotted lower than the corresponding relation indicated in the Specifications for Highway Bridges I (General) [4]. Symptoms of an alkali aggregate reaction were thought to have appeared on part of the beam of specimen S2 due to a significant decline in the modulus of elasticity.

Reinforcing bars and steel plates

Although rust was observed across the entire surface of the sampled reinforcing bars and steel plates there was little decrease in cross section due to corrosion. The yield points of main reinforcing bar, doubly reinforced bar, and steel plate were respectively 291 MPa, 306 MPa, and 398 MPa.

Adhesive

The tensile test of adhesiveness was performed in accordance with JIS K7161 and JIS K7162 (Plastics−Determination of tensile properties). Adhesive was sampled by stripping steel plates off specimens S3 and S4 after completion of the loading test. The dimensions of the tensile test sample were 200 mm (length) × 30 mm (width) × 4 mm (thickness). Results of the tensile test indicated little difference between specimens S3 and S4. The modulus of elasticity and Poisson's ratio (average of values for specimens S3 and S4) were respectively 1.36 GPa and 0.47.

Asphalt layer

The asphalt layer (hereinafter referred to the "As layer") was sampled from specimen S3. Dimensions of the specimen were 30 mm × 40 mm (cross section) and 100 mm (height). Since the material testing of As layer greatly depends on test conditions (temperature and loading velocity), a temperature of 7 C° and the loading velocity of 0.2 mm/minute which were test conditions for the loading test of reinforced concrete beams were adopted. Maximum stress and modulus of elasticity were respectively 6.4 MPa and 3.1 GPa.

<u>Test program</u>

Two-point loading was applied to beams having a span length of 10 m and the shear span of 2 m, corresponding to the support points of the original bridge (Figure 2, Photo 2). Steel plates 200 mm long span-wise and with a thickness of 20 mm were respectively installed at the loading point and the supporting point.

The main measurement items were deflection at midspan, reinforcing bar strain, and steel plate strain. The strain of the main reinforcing bar was measured by chipping the side of concrete directly below the loading point to expose the reinforcing bar and mounting strain gauges on the main reinforcing bar (at two locations on one side of specimens S1 and S2, and at one location on each side of specimens S3 and S4). Clip gauges were installed in order to monitor gaps between the steel plate and concrete and between the steel plate and the splice plate. Specimen S3 was loaded under the condition that there was no asphalt surfacing. The loading test was conducted in winter.

Results

State of joint failure

In the loading test of specimens S1 through S4, deformation such as resin cracking was observed in joints of all specimens. Different failure properties of joints were confirmed depending on whether bolts were added or not.

Since no bolts were added to joints in specimens S1 and S2, taking specimen S1 as an example, the state of the resin cracks in the joints and the splice plate failure are shown in Photo 3(a) and Photo 4. In specimens S1 and S2, resin cracks started at the end of the splice plate for joints. (Such resin cracking is hereinafter referred to as partial splice plate end debonding) In both specimens S1 and S2, the resin cracks subsequently progressed between the splice plate and base members, and more than a half of the splice plate on one side completely debonded from the base members. (This state is called debonding failure of the splice plate, Figure 6(a))

Photo 3(b) shows the state of resin cracks in joints taking specimen S3 as an example. In specimens S3 and S4 where whose joints bolts are added, resin cracks started at the contact between base members. (Such resin cracking is hereinafter referred to as partial debonding due to the contact of base members, Figure 6(b)) Resin cracking subsequently progressed between the splice plate and base members but did not result in debonding failure of the splice plate as in specimens S1 and S2.

Load-deflection curve

Table 1 is a list of the maximum load and the failure type of each specimen, and Figure 7 shows the relation between the load and deflection at midspan. Figure 7 also shows values calculated by the multi-cross section method (detailed below) for a non-strengthened specimen.

Almost identical loads caused partial plate end debonding of the splice plates of joints of specimen S1 and S2 (confirmed by clip gauges). The debonding failure of the splice plate did not occur immediately after partial debonding, and the load on specimens S1 and S2 increased while the rigidity of their girders declined. When debonding failure of the splice plate occurred, the maximum load was reached at a value approximately close to the value calculated value for a non-strengthened specimen. Subsequently, the load on specimens S1 and S2 gradually declined and their deflections increased while a load somewhat lower than the values calculated for a non-strengthened specimen was maintained.

In specimen S3, after partial debonding due to the contact of base members occurring at 374 kN (visuallyconfirmed), the rigidity of its girder gradually declined due to bending cracking of concrete occurring at the partial debonding point. Subsequently, the steel plate near a joint began to gradually debond. At 637 kN, significant debonding occurred at the end of the steel plate as well and the load reached the maximum.

Partial debonding due to the contact of base members occurred at 407 kN with

Specimen S4 (visually confirmed). At 568 kN, the steel plate drastically debonded from the cover concrete, from its end to the vicinity of the center of the specimen along the crack at the location of the lower main reinforcing bar (Photo 5), with the load sharply declining to about 400 kN. The specimen was then unloaded and loaded again with the cover concrete delaminated. After reaching the maximum load, specimens S3 and S4 exhibited behavior mostly similar to that corresponding to the value calculated for a non-strengthened specimen just the same as for specimens S1 and S2. In both specimens S3 and S4, yielding on the main reinforcing bar was observed after the maximum load was reached. On specimens S3 and S4, the addition of bolts reduced the debonding failure of the splice plate.

Plate end debonding of the steel plate on specimen S3 occurred at the interface between the steel plate and concrete. The steel plate was stripped off after the loading test to observe the bonded surface. Rust was found to have developed on most of the surface, but no adhesive was found adhering to the steel plate. This suggests the possibility that adhesion loss was caused by water leakage that resulted in rust formation on the steel plate, causing a decrease in adhesive area on the steel plate which mainly caused debonding failure of the steel plate and the resin layer.

On specimen S4, stripping off the steel plate to observe the bonded surface revealed that delamination of cover concrete had occurred despite rust formation on its main section. Such a failure is often observed in loading tests on steel plate reinforced concrete girders which have shear reinforcing bars(Figure 1 (b)). The reason why delamination of cover concrete occurred is considered to be the effect of cracks along the main reinforcing bar observed before loading.

Axial strain distribution of the steel plate

Figure 8 shows the axial strain distribution on steel plate immediately before the partial debonding of the splice plates of joints on specimens S1 and S2 and immediately before partial debonding due to the contact of base members in specimens S3 and S4. Values calculated by the multi-cross section method for specimens strengthened by an integrated steel plate over its full length are also shown in the figure.

While measured strains of specimens S1, S3, and S4 generally tended to coincide with calculated values except for joints, the measured strain on specimen S2 were generally lower than the calculated values.

<u>Influence effect of bonded steel plate joint on load-carrying properties of reinforced concrete girders</u>

Numerical calculation

Figure 9 shows the flow chart for calculation. In order to evaluate load-carrying properties in terms of the effect on joints of reinforced concrete girders strengthened with externally bonded steel plates, numerical calculation was conducted by the multi-cross section method while taking the effects on steel plate joints into account.

The result of the material test was used as the material model in this calculation. The stress-strain relation from results of the compressive strength test was utilized on the compressive side as the stress-strain relation for concrete. The Okamura-Maekawa model[5]) was used for tension stiffening after the initiation of cracks on the tensile side. A bilinear model disregarding the strain hardening area was used for the stress-strain relation of reinforcing bars. The stress-strain relation from the compressive strength test was used on the As layers. The steel plate was modeled by dividing into general and joint sections. The stress-strain relation from the tensile test of steel plates was utilized for the general section, and the stress-strain relation of the center of the joint section (detailed below) was used for the joint section. The 1/2 Beam Model which axially divides the modeled object into two parts is used as the calculation model. To obtain a stable solution for element breakdown, the cross section of a specimen was divided into 50 elements and the support point to the loading point into 50 elements.

Stress-strain relation for the joint section

In the static tensile test of single-spliced bolted adhesive joints having physical details equivalent to those of steel joints on reinforced concrete girders used in the bending loading test (Photo 6) [6]; bending deformation occurred due to an eccentricity specific to a single-sided splice. Partial debonding (peeling or delaminating) occurred at a relatively early stage at the contact of abutting base members and the splice plate ends (Figure 10). At that time, the load did not decrease immediately and a significant increase in deflection was observed. In the static tensile test of unbolted adhesive joints, the initiation of partial debonding of the splice plate in the joint section did not immediately result in whole surface debonding and the load was held despite partial debonding occurring three or four times.

Figure 11 represents these behaviors in terms of a stress-strain relation. Specimens S1 and S3 in the figure as examples, in calculating the unit stress of the steel plate upon the occurrence of partial debonding, the unit stress acting on the center of the joint section was calculated on the basis of the load at the occurrence of partial debonding by using the beam bending theory. The upper strain limit during the period from the occurrence of partial debonding of splice plates to their total debonding in the joint section was tentatively set at 800 μ so that it generally coincides with the experimental value of the maximum load (Figure 11(a)).

Calculation results and discussion

Figure 7 shows the result of applying the proposed model of stress-strain relation for the joint section into the numerical calculation by the multi-cross section method (Figure 9) and performing the calculation.

The values calculated for specimens S1 and S2 transition to those for a non-strengthened specimen due to total loss of the strengthening effect of the steel plates resulting from total debonding of splice plates in the joint section. Values calculated for

specimens S1 and S2 mostly exhibited behavior similar to that corresponding to experimental values for the period from occurrence of partial debonding on splice plates to a decline in girder rigidity.

Values calculated for girder rigidity and the maximum load for specimen S3 (Case 1) were greater than the corresponding experimental values. While partial debonding due to the contact of base members was visually confirmed during the experiment, symptoms of partial debonding might have actually appeared at an earlier stage. Therefore, in order to examine the impact of such partial debonding, the calculation was made on the basis of a model using unit stress (measured value) calculated by multiplying the strain of the center of one of two joint sections in specimen S3 shown in Figure 8(b) in which partial debonding occurred earlier (shown on the left in the figure), by the modulus of elasticity of the steel plate. The result of this calculation mostly coincided with experimental values up to the clear occurrence of debonding from the ends of the steel plates. Though we were unable to visually confirm the difference between calculated and measured values at and after the deflection of 20 mm, that this might be the result of gradual debonding.

Values calculated for specimen S4 generally coincided with experimental values up to the peak value. Experimental values for specimen S4 did not reach the calculated peak value due to a drastic gradual progression of debonding from the ends of steel plates.

Calculatied results for specimen S3 and S4 show a tendency where the maximum load is capped even if the strength of joints improves, because partial debonding due to the contact of base members of steel plates occurs at a relatively early stage due to the effects of eccentricities specific to the structure of single-spliced joints.

Load when plate end debonding occurs

In specimens S3 and S4 debonding failure started at the ends of the steel plate. An analysis method for estimating the state of stress for debonding failure at the end of reinforcing material such as steel plates and FRP has been proposed by Roberts[7]. A model for checking debonding failure corresponding to the stress state of reinforcing material has been proposed by Tumialan et al.[8] The model calculates the maximum principal stress on concrete near the ends of the reinforcing material by substituting shear stress (τ), bending tensile stress (σ_x), and tensile stress acting on the ends of the reinforcing material (σ_y) into the equation (1) based on the stress state of the ends of the reinforcer estimated on the basis of Roberts's approximate solution. According to the model, debonding failure occurs at the ends of the reinforcing material if the calculated value is greater than the tensile strength of the concrete (f_t).

$$\sigma = \frac{\sigma_x + \sigma_y}{2} + \sqrt{\left(\frac{\sigma_x - \sigma_y}{2}\right)^2 + \tau^2} \geq f_t \quad (1)$$

Table 1 shows results from calculating (Figure 9) the load during plate end debonding using the maximum stress obtained from a theoretical formula based on the model from Tumialan et al.

Conclusions

A stress-strain relation model for joints was applied to the numerical calculation using the multi-cross section method to compare the calculated values with experimental results. Results showed a decline in the rigidity of girders after occurrence of partial debonding of the splice plates of the joint was successfully represented by applying the model. Also revealed was that the maximum load is capped even if the joint strength improves due to effects from an eccentricity specific to the structure of single-spliced joints. The experiment using bolts to improve the joints ended before reaching the maximum load for that coupling due to the occurrence of plate end debonding. In view of this result, it is necessary not only to check plate end debonding but also the impact of single-sided adhesive joints in evaluating the load-carrying capacity of reinforced concrete girders on currently used highway bridges that were strengthened with externally bonded steel plates.

Acknowledgments

References

[1] Jones, R., Swamy, R. N., Bloxham, J., and Bouder, Balah, A., Composite behaviour of concrete beams with epoxy bonded external reinforcement, Int JCem Compos, 2(2), pp.91-107, 1980.
[2] Yoshida, E., Murakoshi, J., Kimura, Y., and Tanaka, Y., Load-carrying Capacity Test of Deteriorated Reinforced Concrete Girders Strengthened by Externally Bonded Steel Plates, Proc. JSCE Annual meeting, V-189, pp.377-378, 2011. (in Japanese)
[3] Yoshida, E., Murakoshi, J., Kimura, Y., Tanaka, Y., Iizuka, T., Load-carrying Capacity Test of Reinforced Concrete Girders Strengthened by Externally Bonded Steel Plates with Bolted Adhesive Joints, Proc. JSCE Annual meeting, V-180, pp.359-360, 2013. (in Japanese)
[4] Specifications for Highway Bridges and their Commentary, Japan Road Association, Mar. 2012.
[5] Okamura, H., and Maekawa, K., Nonlinear Analysis and Constitutive Models of Reinforced Concrete, Gihodoshuppan, May 1991
[6] Iizuka, T., Murakoshi, J., and Tanaka, Y., Examination of the Method to Improve Joints for Strengthening Reinforced Concrete Girders by Externally Bonded Steel Plates, Proc. JSCE Annual meeting, I-343, pp.685-686, 2012. (in Japanese)
[7] Roberts, T. M., Approximate analysis of shear and normal stress concentrations in the adhesive layer of plated RC beams, Structural Engineer, 67(12), pp.229-233, 1989.
[8] Tumialan, J. G., Belarbi, A., and Nanni, A., Reinforced Concrete Beams Strengthened with CFRP Composites: Failure due to Concrete Cover Delamination, Center for Infrastructure Engineering Studies, 99-01, Department of Civil Engineering, Univ. of Missouri - Rolla, March 1999.

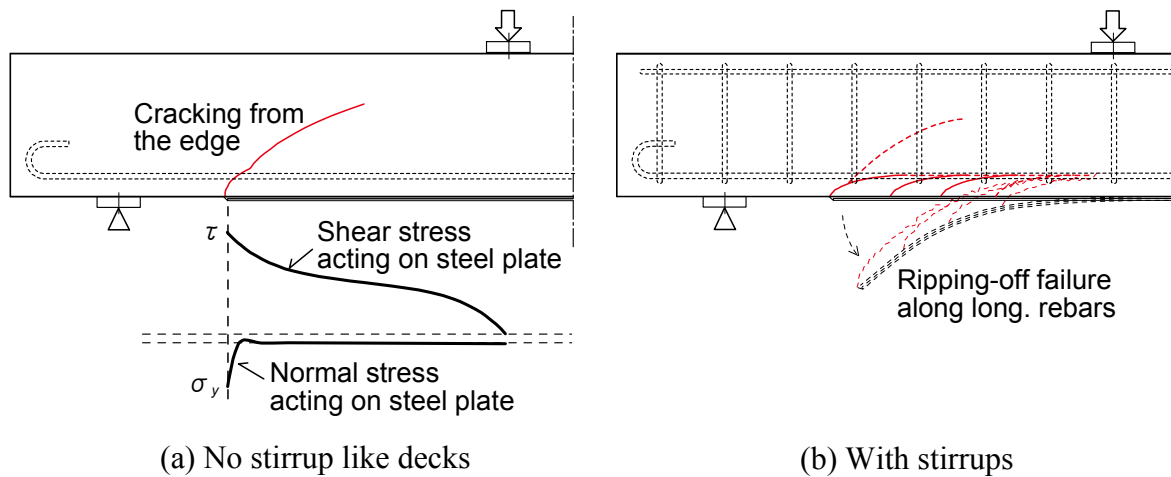Photo 1 Steel plates bonded to the soffit of girders
in a concrete bridge

τ

Cracking from
the edge

Shear stress
acting on steel plate

σ_y

Normal stress
acting on steel plate

Ripping-off failure
along long. rebars

(a) No stirrup like decks

(b) With stirrups

Figure 1 Types of Failure of Plated Beam

Table 1 Maximum Load, Calculated Values, and Failure Type of Specimens

Specimen	Max. load (kN)				Measured value/calculated value for non-strengthened specimen	Joint strengthened	Asphalt paved	Failure type
	Measured value	Calculated value for non-strengthened specimen	Calculated value for a strengthened specimen	Calculated value for a specimen at time of plate end debonding				
S1	519	502	512[*1]	-	1.04	No	Yes	A
S2	478	501	493[*1]	-	0.95	No[*3]	Yes	A
S3	637	502	659/628[*2]	591	1.27	Bolt added	No[*4]	B
S4	568	503	688	584	1.13	Bolt added	Yes	B

*1: Considering total surface debonding of splice plate of a joint.*2: Case 1 /Case 2.*3: Two joints were vertically restrained by using a tendon bar (axial force per joint was 80 kN), but no effect was observed [2].*4: Beams collapsed due to an earthquake, and asphalt pavement peeled away. A: Debonding failure of splice plate for a joint B: Steel plate end debonding

: Debonding area of reinforcing steel plate confirmed before experiment

: Debonding area of reinforcing steel plate confirmed after completion of experiment
(excluding position of the steel plate anchor)

— : Existing cracks — : Cracks upon loading

○ : Location of cores sampled from the side of the web ▭ : Location of cores sampled from the cross section
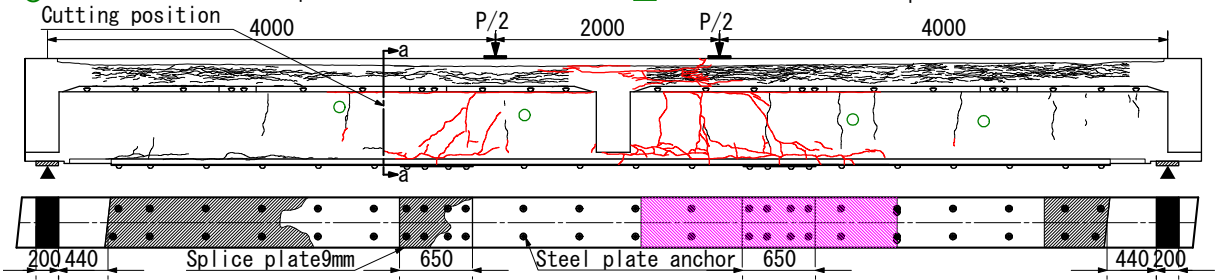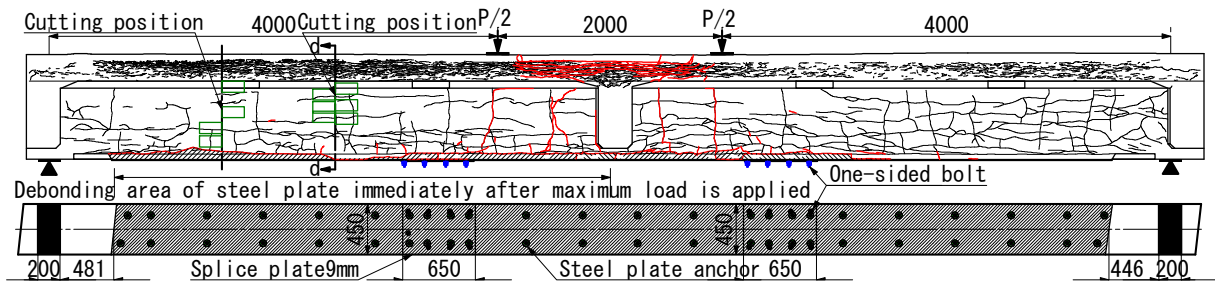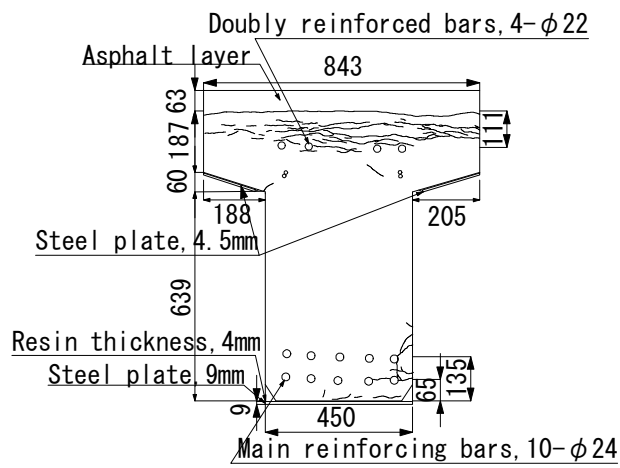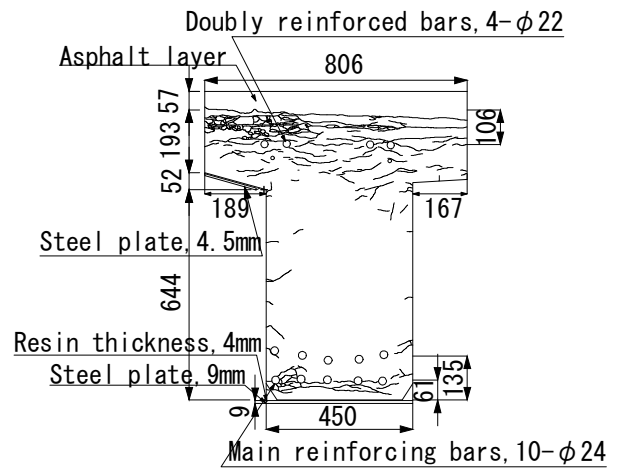
(a) Specimen S1
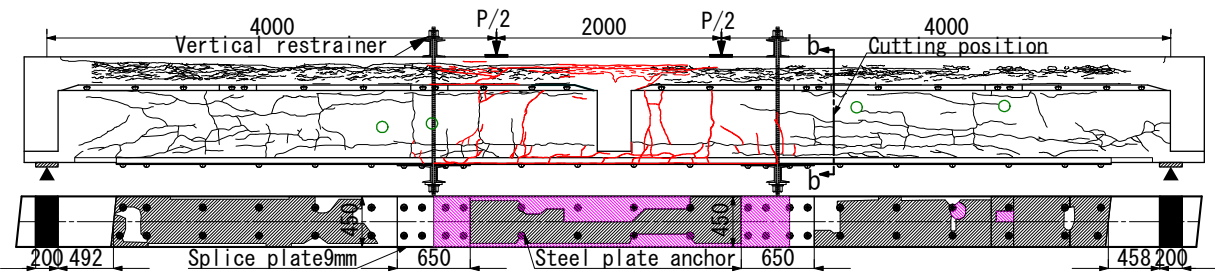
(b) Specimen S2
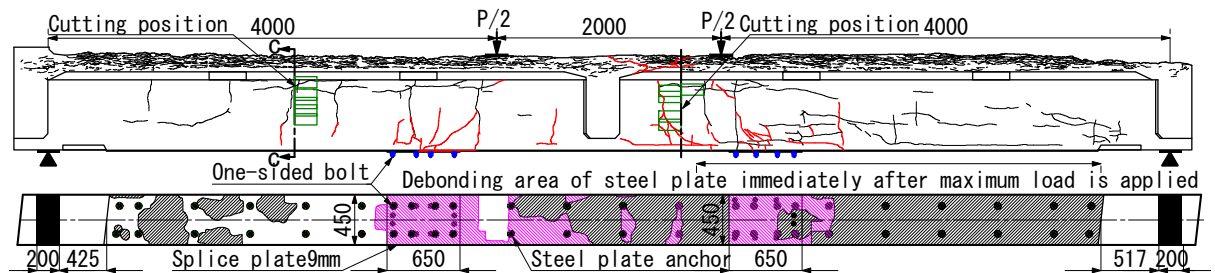
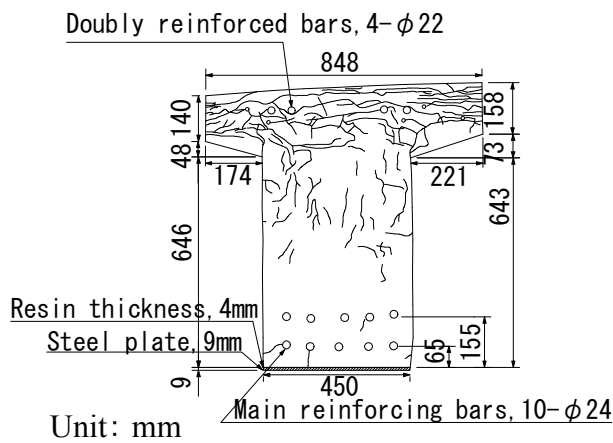(c) Specimen S3

Unit : mm

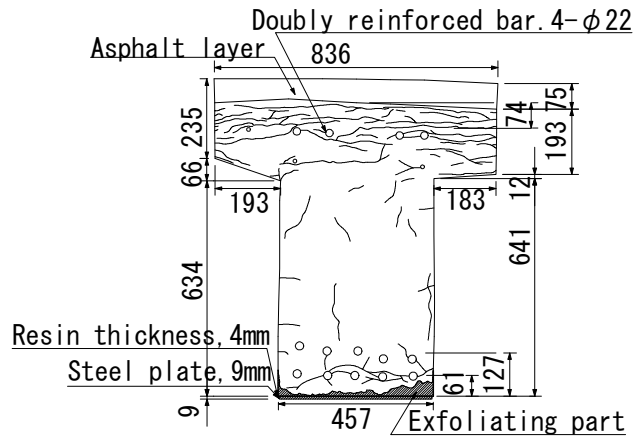(d) Specimen S4

Figure 2 Appearance before and after loading test

(a) Cross section a-a

(b) Cross section b-b

(c) Cross section c-c

Unit: mm

(d) Cross section d-d

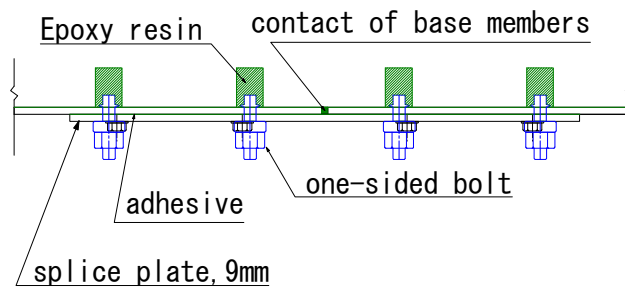Figure 3 Cross section after loading test

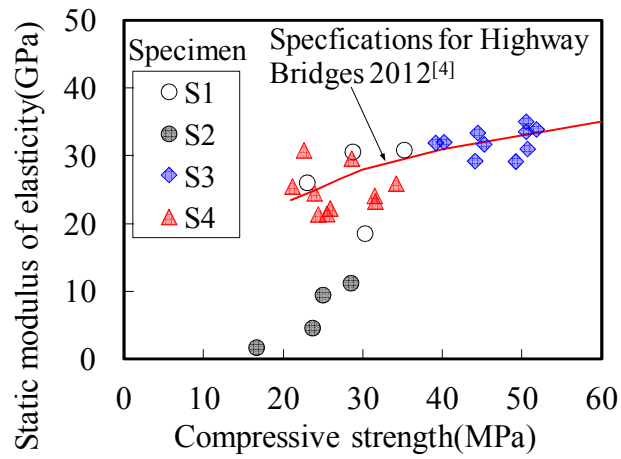Figure 4 Detailed drawing of joint after bolt insertion

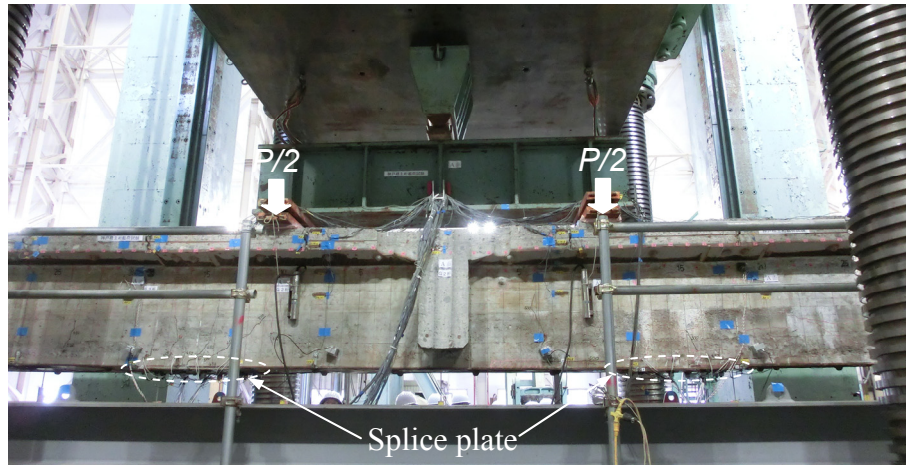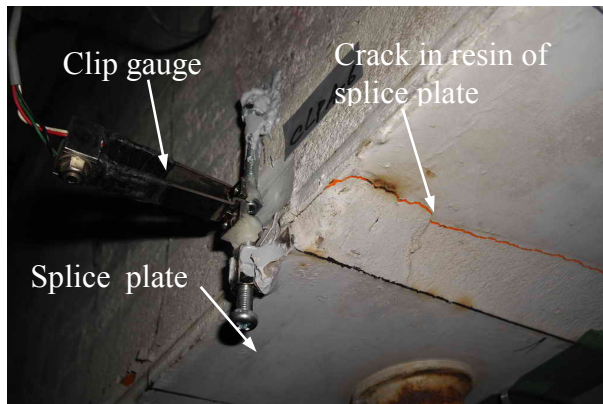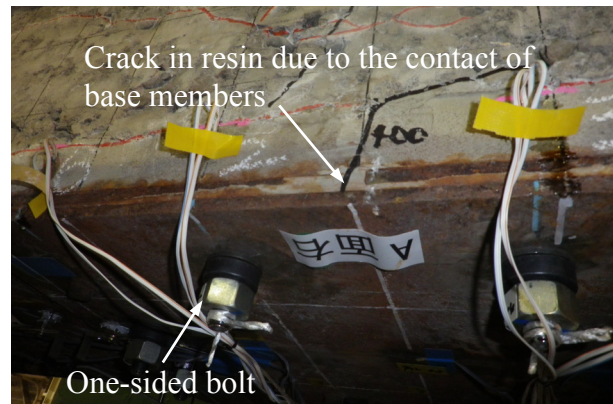Figure 5 Result of concrete core compressive strength test

Photo 2 Bending Status of the test

(a) Specimen S1

(b) Specimen S3

Photo 3 Resin cracks on joint (specimens S1 and S3)

━ : Starting point of resin crack
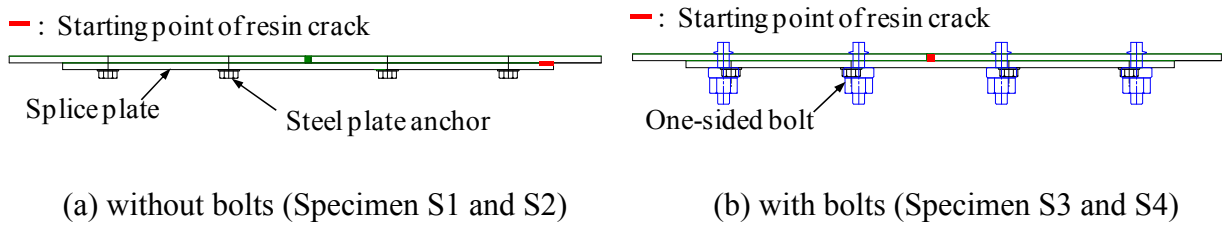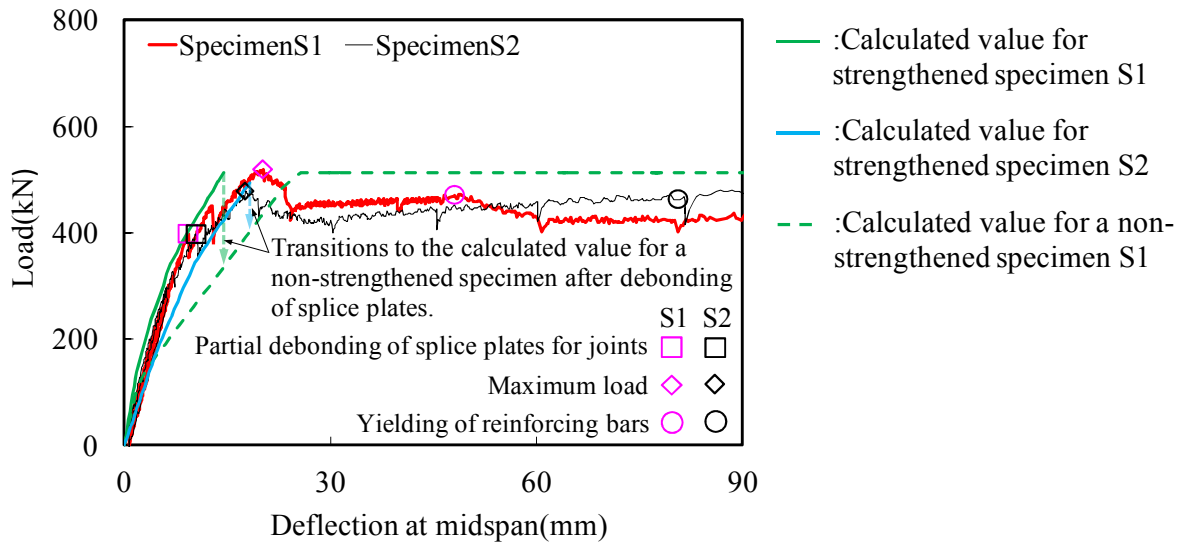
Splice plate

Steel plate anchor

One-sided bolt

(a) without bolts (Specimen S1 and S2)   (b) with bolts (Specimen S3 and S4)

Figure 6 Resin cracks on joint

── SpecimenS1 ── SpecimenS2

── :Calculated value for strengthened specimen S1

── :Calculated value for strengthened specimen S2

╌╌ :Calculated value for a non-strengthened specimen S1

Transitions to the calculated value for a non-strengthened specimen after debonding of splice plates.

	S1	S2
Partial debonding of splice plates for joints	□	□
Maximum load	◇	◇
Yielding of reinforcing bars	○	○

(a) Specimen S1 and S2

── SpecimenS3 ── SpecimenS4

── :Calculated value for strengthened specimen S3 (Case1)

── :Calculated value for strengthened specimen S3 (Case2)

── :Calculated value for strengthened specimen S4

╌╌ :Calculated value for a non-strengthened specimen S3

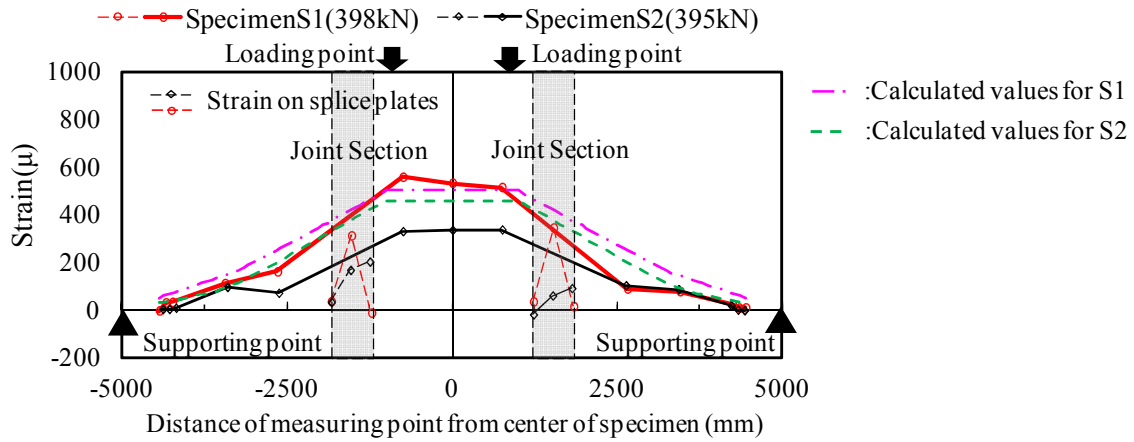|	S3	S4
Partial debonding due to the contact of base members	□	□
Maximum load	◇	◇
Yielding of reinforcing bars	○	○

(b) Specimen S3 and S4

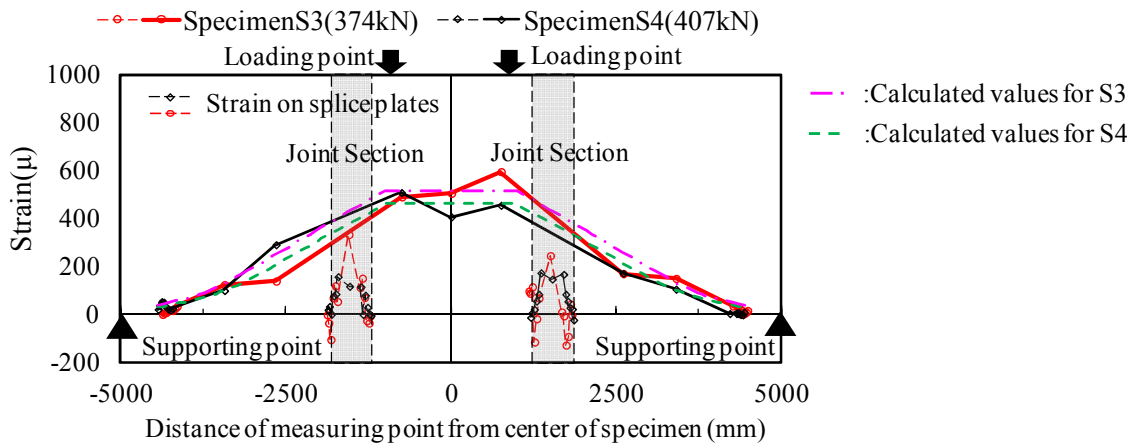Figure 7 Relationship between load and deflection at midspan

Photo 4 Debonding failure of splice plates on specimen S1

Photo 5 Debonding failure from ends of steel plate (near side in the photo) of specimen S4 (immediately after maximum load is applied)

（a）Specimens S1 and S2

（b）Specimens S3 and S4

Figure 8 Distribution of axial strain of the steel plate

START

Enter member dimensions and material property values of materials (including joints)

Set the strain ε_c of the extreme compression fiber of concrete

Increment of ε_c

Set the depth of the neutral axis x

Reconfigure x

Calculate the strain of an element ε_i

Calculate the stress of each element corresponding to ε_i

Calculate the sectional force N_i of each element

Resultant force of members $\Sigma N_i = 0$

No

Yes

Calculate bending moment M: curvature Φ

$\varepsilon_c \leqq$ concrete crushing strain ε_{cu} *1

No

Yes

Calculate M_u, P_u *2

Integrate M-Φ over the span direction *3

Increment of P

Calculate deflection δ

$P \leqq P_u$

No

Yes

END

※1: ε_{cu}=3500μ.
※2: M_u: bending moment corresponding to ε_{cu}
P_u: concrete crushing load (=2M_u/a)

*3: 1/2 Beam Model (schematic diagram)

a=4000

P/2 1000^{CL}

x_1 x_2 • • • • x_{43} • • x_{50}

○ :Element

General section

Joint section

- - - : Flow for calculating load causing debonding on plate end

Calculate the maximum principal stress σ at time of debonding failure on steel plate end

Increment of P

$\sigma \geqq$ tensile strength of concrete f_t

No

Yes

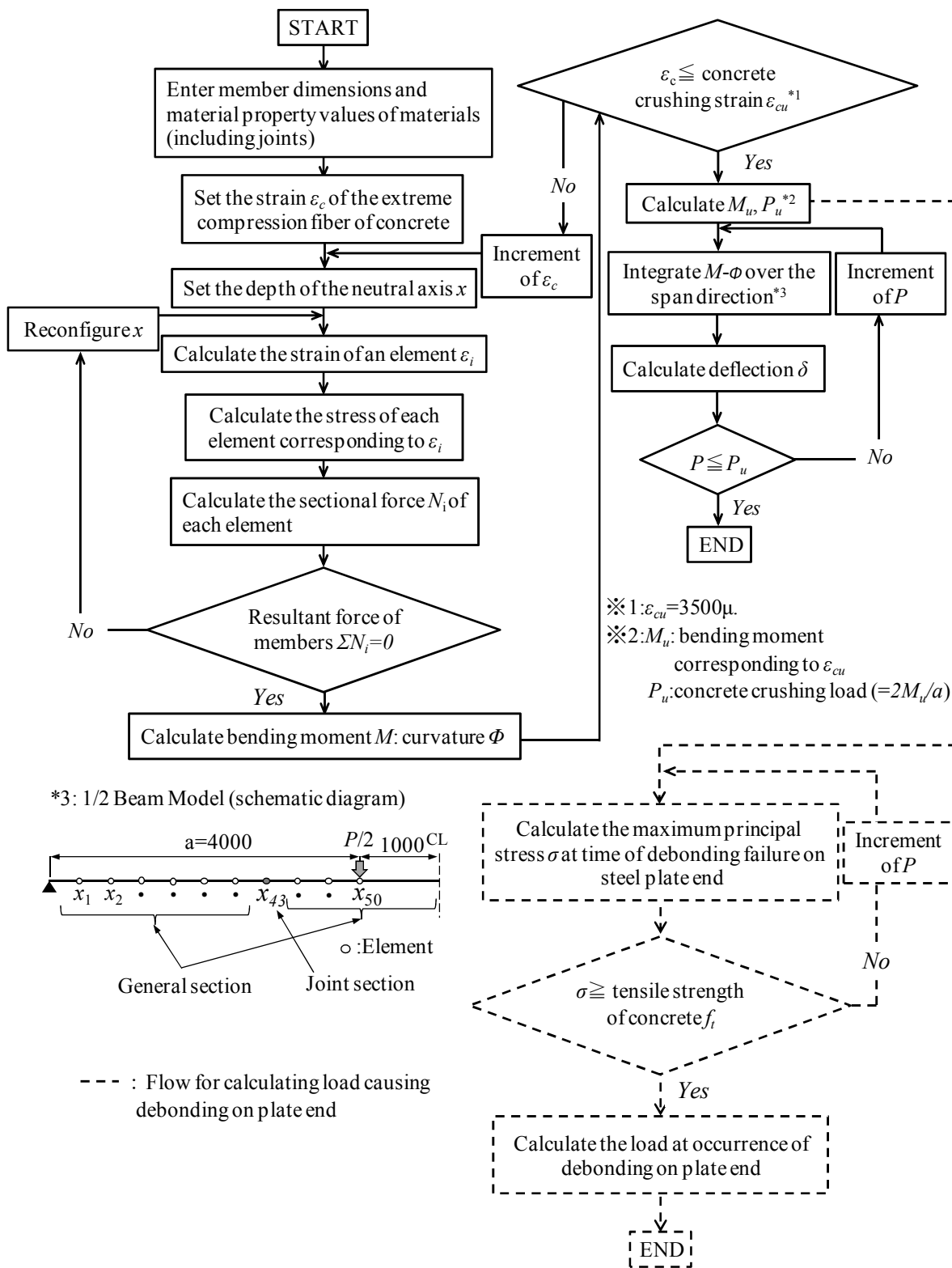Calculate the load at occurrence of debonding on plate end

END

Figure 9 Flow chart for calculation

Photo 6 Static tensile test of single-spliced
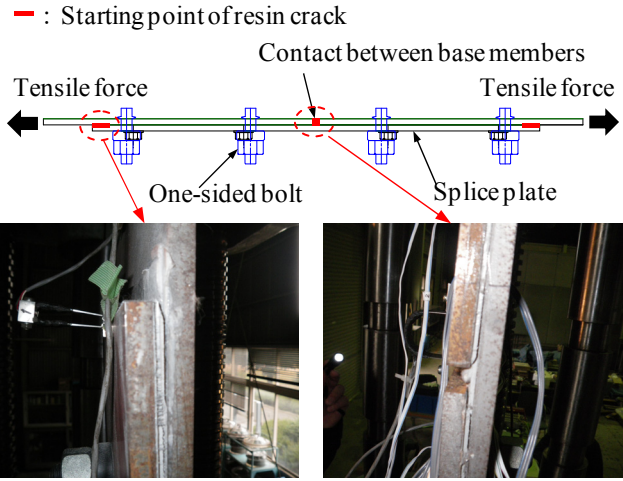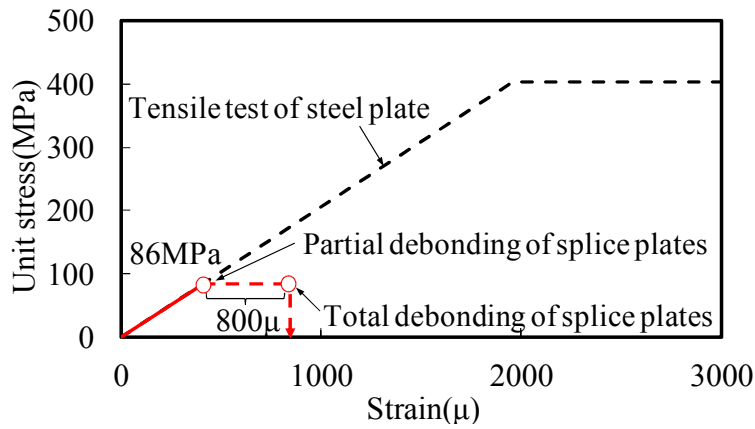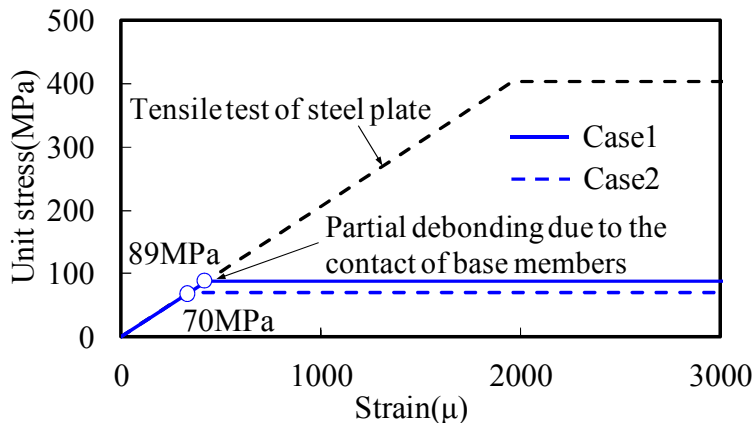bolted adhesive joints[6)]

Figure 10 Failures observed in static tensile test
of single-spliced bolted adhesive joints

(a) Specimen S1 (without bolts)

(b) Specimen S3 (with bolts)

Figure 11 Schematic diagram of the stress-strain relationship in the center of joints